Electronic Supplementary Material (ESI) for Physical Chemistry Chemical Physics.

Supporting information

Experimental and Computational Methods

IRPD spectroscopy

The experimental setup and IRPD scheme have been described previously (Figure S1).[1, 2] A methanol solution of benzocaine (BC, Wako, 3.0×10^{-4} M) with 0.5 % (v/v) of formic acid was electrosprayed from an emitter. Fine droplets generated by electrospray were desolvated in a glass capillary heated up to ~80 °C. The generated ions were introduced into vacuum via an ion funnel. The ions of interest were mass-selected by a quadrupole mass spectrometer (QMS) and transported by a tapered hexapole ion guide. The ions were hydrated in a linear octupole ion trap (LIT[2, 3]), in which the vapor of water was introduced by a pulsed valve. The temperature of the LIT was kept at 170 K. The ions were stored in the LIT for a long duration (50 ms) to reach thermal equilibrium. Hydrated ions were mass-selected by a second QMS and introduced into a cold quadrupole ion trap (QIT) via a quadrupole ion deflector and octupole ion guides. The QIT was kept at 4 K by a closed-cycle two-stage He refrigerator (Sumitomo, RDK-408D2). Helium buffer gas was introduced into the QIT by a pulsed valve to collisionally cool the hydrated ions down to ~10 K. The cold hydrated ions were irradiated with a tunable OPO/OPA IR laser. The photofragments generated by the dissociation of water molecules (n>1) or H_2 (n=0) were monitored by a time-of-flight mass spectrometer. The IRPD spectra were measured by scanning the yield of the photofragment ions as a function of laser wavenumber.

CAS-IRPD spectroscopy

Hydrated ions were guided to the QIT with a high kinetic energy (~16 eV) by lowering the offset voltage of the entrance electrode of the QIT. This kinetic energy is significantly higher than the one used for conventional IRPD spectroscopy (typically 2 eV) in this setup. The ions were allowed to dissociate into bare H^+BC and H_2 molecules were attached to H^+BC. The H_2-detached photofragments were detected while scanning the wavenumber of the IR laser.

Theoretical calculations

Molecular structures and vibrational frequencies of $H^+BC(H_2O)_n$ were calculated with density functional theory (DFT). DFT calculations were performed with the Gaussian 16 software[4] using the dispersion-corrected ωB97X-D/6-311++G(d,p) level.[5] Relative Gibbs free energies at 298 K were calculated at the same level. The initial structures of $H^+BC(H_2O)_n$ were automatically generated by adding a water molecule to all possible binding sites (OH and NH) of $H^+BC(H_2O)_{n-1}$ using a homemade Python program. All calculated conformers shown were confirmed to be local minima on the potential energy surface (without any imaginary vibrational frequency). Obtained harmonic vibrational frequencies were scaled by 0.952.[6] For the most stable protomer, the Gibbs free energy calculation was re-performed at 170 K. We also performed DFT calculations at the M06-2X/6-311++G(d,p) or B3LYP-D3/6-311++G(d,p) levels and *ab initio* calculations at the MP2/cc-pVTZ level using the most stable isomer as initial structure. The IR spectra of H_2-tagged H^+BC were also calculated (Figure S11) and

show that the N-protomer tagged with three H_2 ligands gives the best match with experimental CAS-IRPD spectra. We employed the IR oscillator strength of $H^+BC\text{-}(H_2)_3$ for the analysis of the CAS-IRPD spectra.

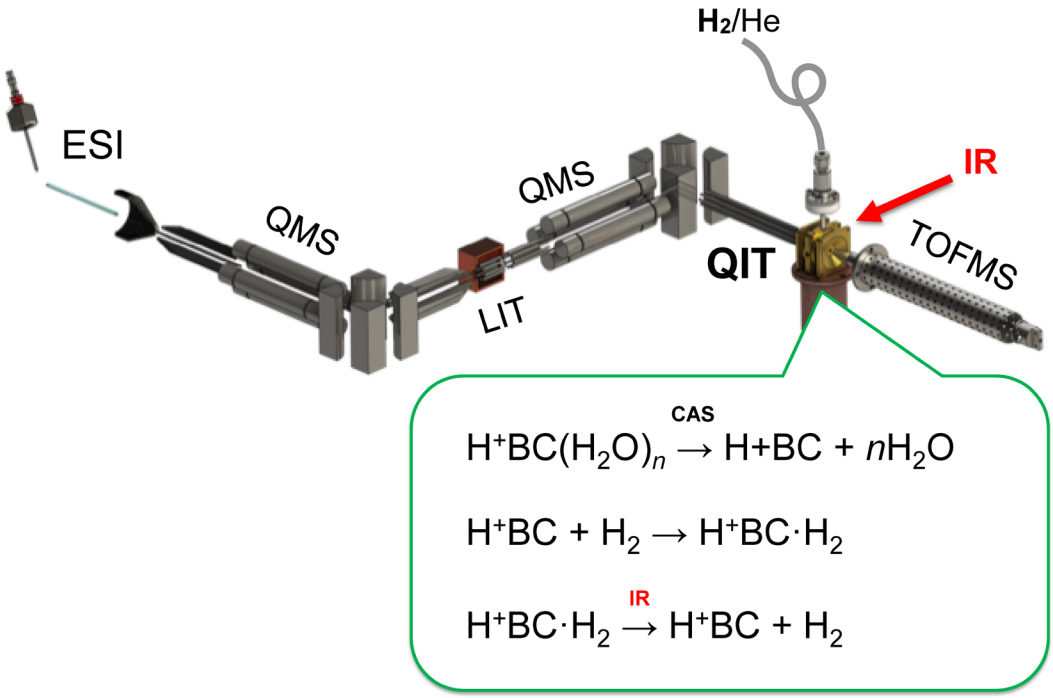

Figure S1. Experimental setup. ESI: Electrospray ionization, QMS: Quadrupole mass spectrometer, LIT: Linear ion trap, QIT: Quadrupole ion trap, TOFMS: Time-of-flight mass spectrometer, CAS: Collision-assisted stripping.

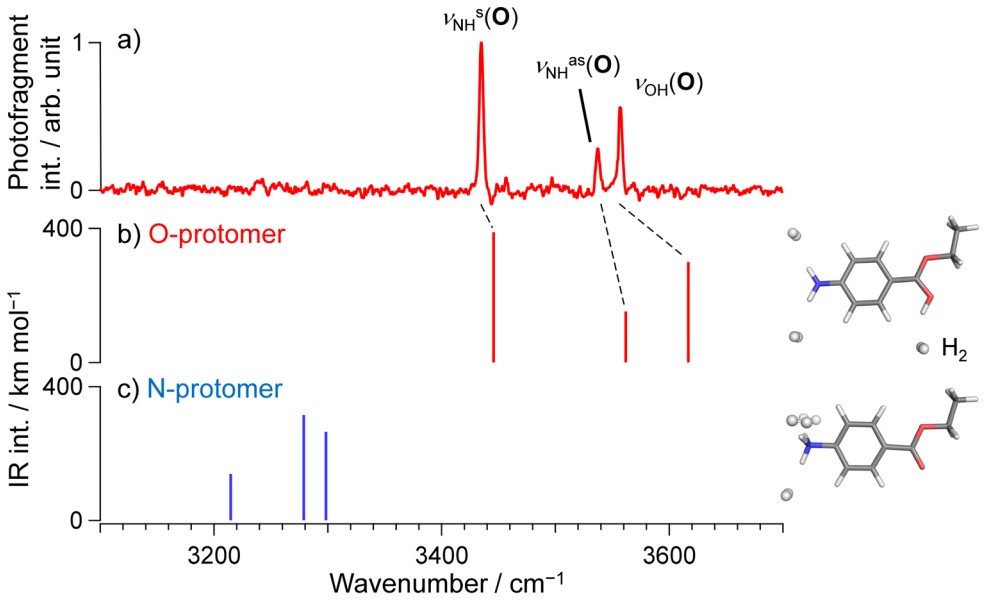

Figure S2. a) IRPD spectrum of protonated benzocaine (H^+BC) and theoretical IR spectra of the most stable b) O- and c) N-protomers. The theoretical spectra were calculated for the H_2-clusters where three H_2 molecules are attached to H^+BC.

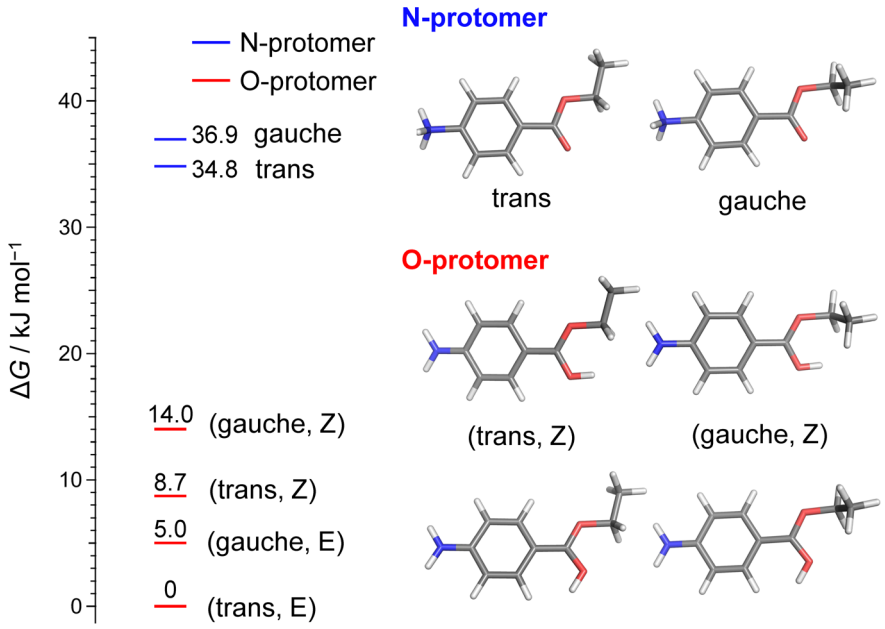

Figure S3. Gibbs free energies of the conformers of H^+BC at the ωB97X-D/6-311++G(d,p) level at 298 K. The term *trans* or *gauche* is defined by the orientation of the ethyl moiety. The term *E* or *Z* is defined by the orientation of the OH moiety in the O-protomer.

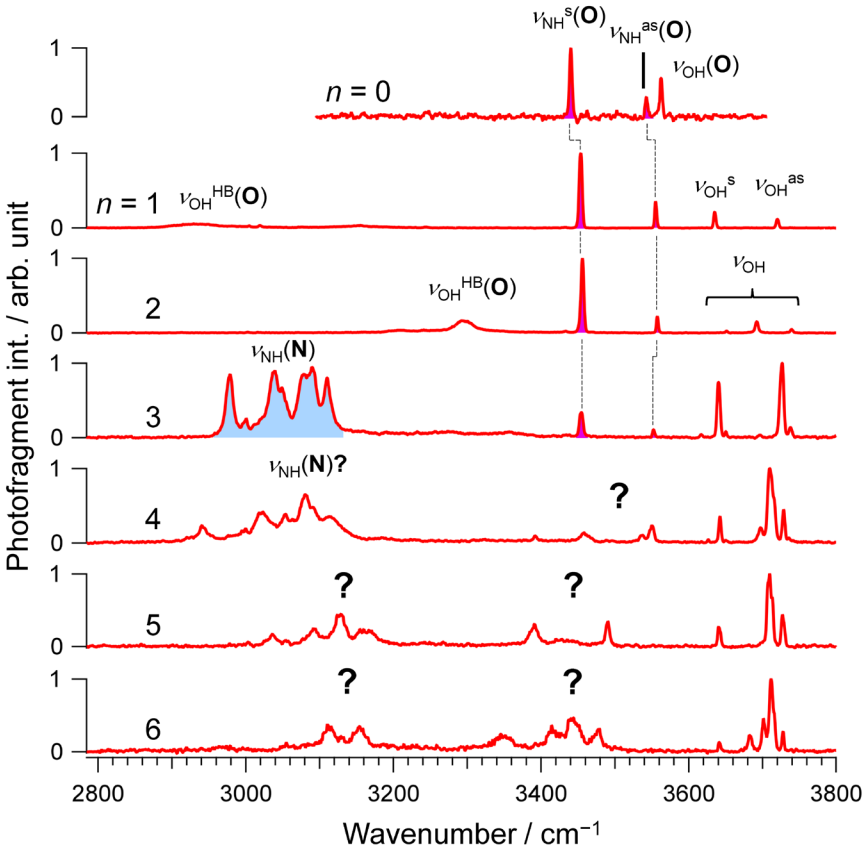

Figure S4. IRPD spectra of $H^+BC(H_2O)_n$ (n=0–6). The question marks in the n=4-6 spectra indicate the problems of vibrational and isomer assignments arising from spectral congestion. The red and blue-colored areas correspond to vibrational bands derived from O- and N-protomers, respectively.

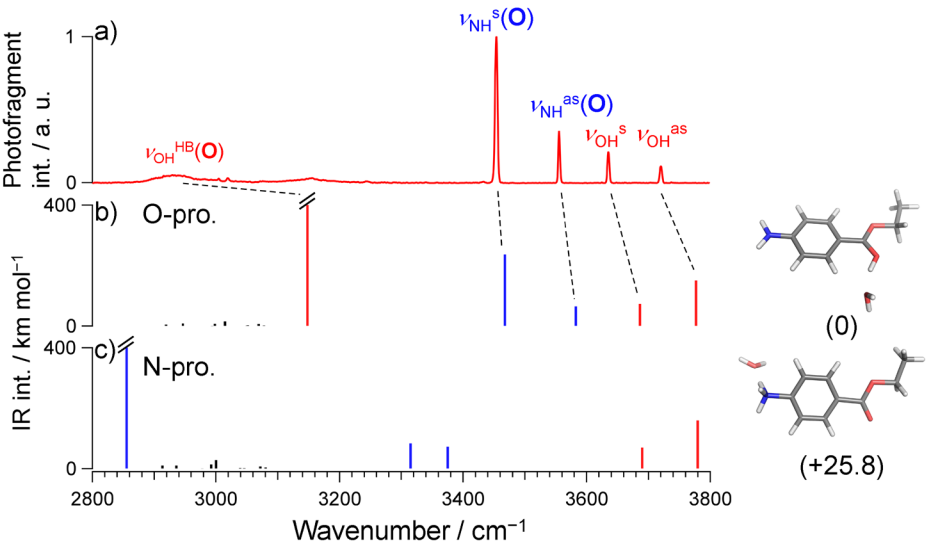

Figure S5. a) IRPD spectra and theoretical IR spectra of the most stable b) O- and c) N-protomers of $H^+BC(H_2O)_1$. The red and blue lines correspond to OH and NH stretches, respectively. Numbers in parentheses indicate relative Gibbs free energies at 298 K in kJ mol^{-1}.

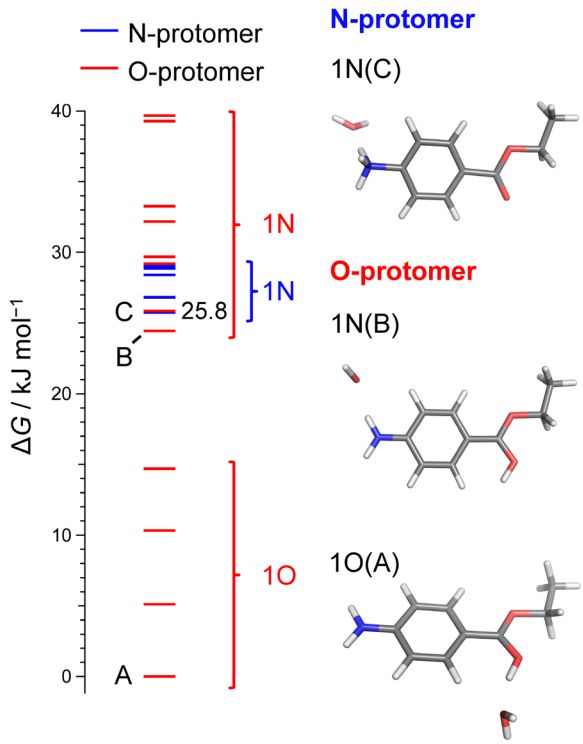

Figure S6. Gibbs free energies of the conformers of $H^+BC(H_2O)_1$ calculated at the ωB97X-D/6-311++G(d,p) level at 298 K. We denote a structure, where the OH(NH) site is hydrated by a water molecule, as 1O(1N). Representative conformations, A, B, and C are shown.

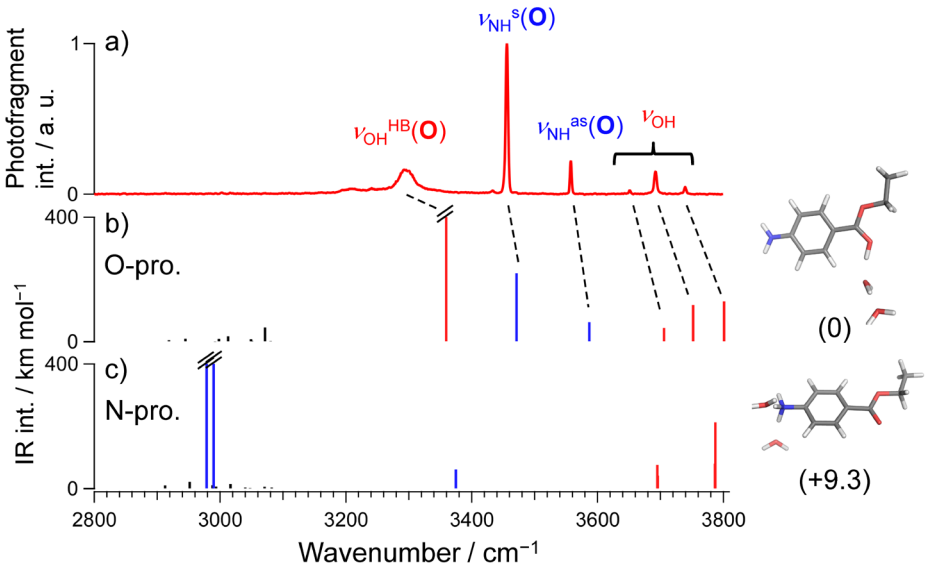

Figure S7. a) IRPD spectra and theoretical IR spectra of the most stable b) O- and c) N-protomers of $H^+BC(H_2O)_2$. The red and blue lines correspond to OH and NH stretches, respectively. Numbers in parentheses indicate relative Gibbs free energy at 298 K in kJ mol^{-1}.

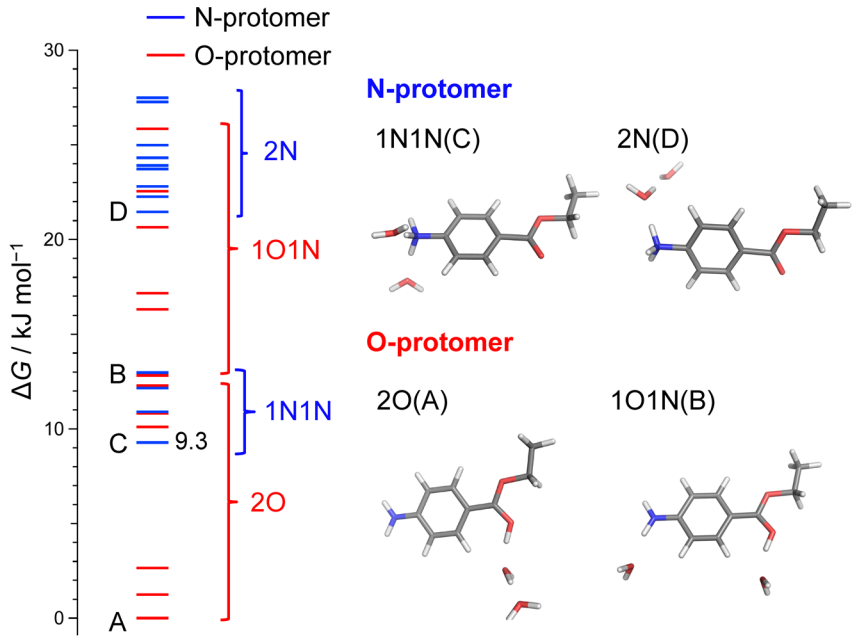

Figure S8. Gibbs free energies of the conformers of $H^+BC(H_2O)_2$ calculated at the ωB97X-D/6-311++G(d,p) level at 298 K. We denote a structure, where the OH(NH) site is hydrated by two water molecules, as 2O(2N). 1N1N indicates a structure where two NH sites are hydrated by a single water molecule. In a 1O1N structure, the OH and one NH site are hydrated. Representative conformations, A, B, C, and D are shown.

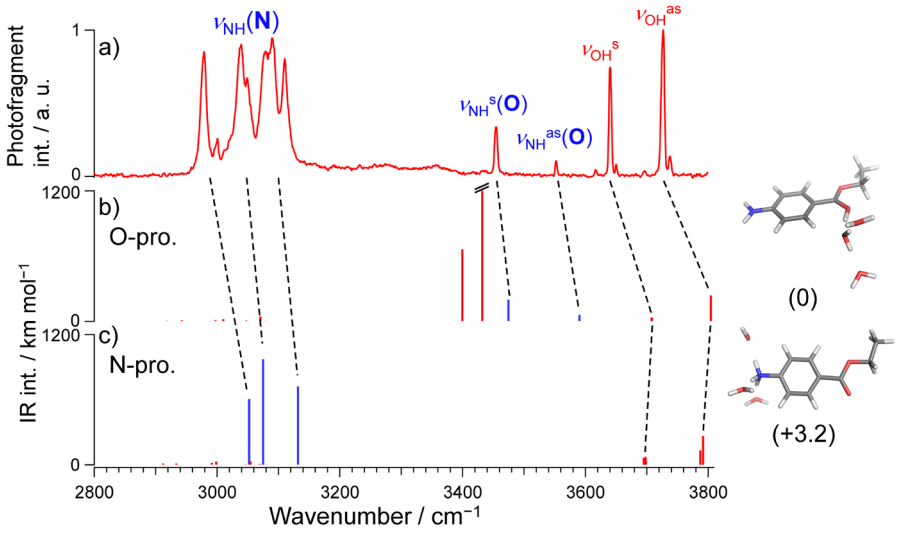

Figure S9. a) IRPD spectra and theoretical IR spectra of the most stable b) O- and c) N-protomers of $H^+BC(H_2O)_3$. The red and blue lines correspond to OH and NH stretches, respectively. Numbers in parentheses indicate relative Gibbs free energy at 298 K in kJ mol^{-1}. We estimated the relative abundance between protomers using ν_{NH}(**N**) (exp: 2979 cm^{-1}, calc: 3052 cm^{-1}, 605 km mol^{-1}) and ν_{NH}^{s}(**O**) (exp: 3455 cm^{-1}, calc: 3475 cm^{-1}, 199 km mol^{-1}). We avoided to use ν_{OH}^{HB}(**O**) (due to band broadening) and the other ν_{NH}(**N**) bands (due to band splitting probably derived from coupling with CH stretches).

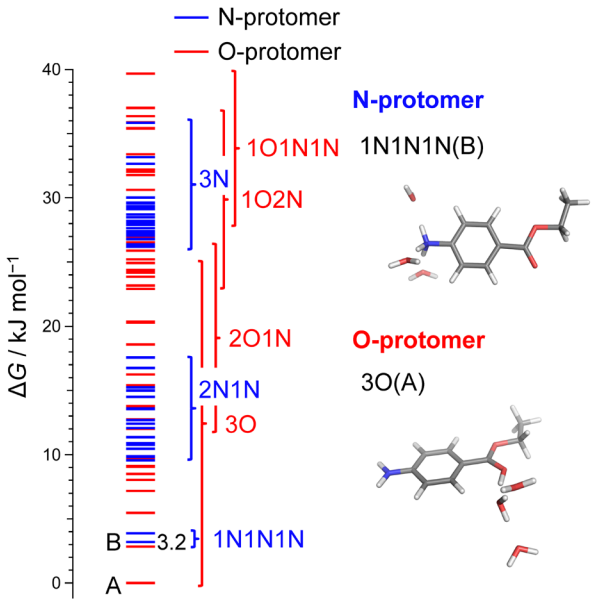

Figure S10. Gibbs free energies of the conformers of $H^+BC(H_2O)_3$ calculated at the ωB97X-D/6-311++G(d,p) level at 298 K. We denote a structure, where the OH site is hydrated by three water molecules, as 3O. 1N1N1N indicates a structure, where the three NH sites are hydrated by a single water molecule. Representative conformations A and B are shown.

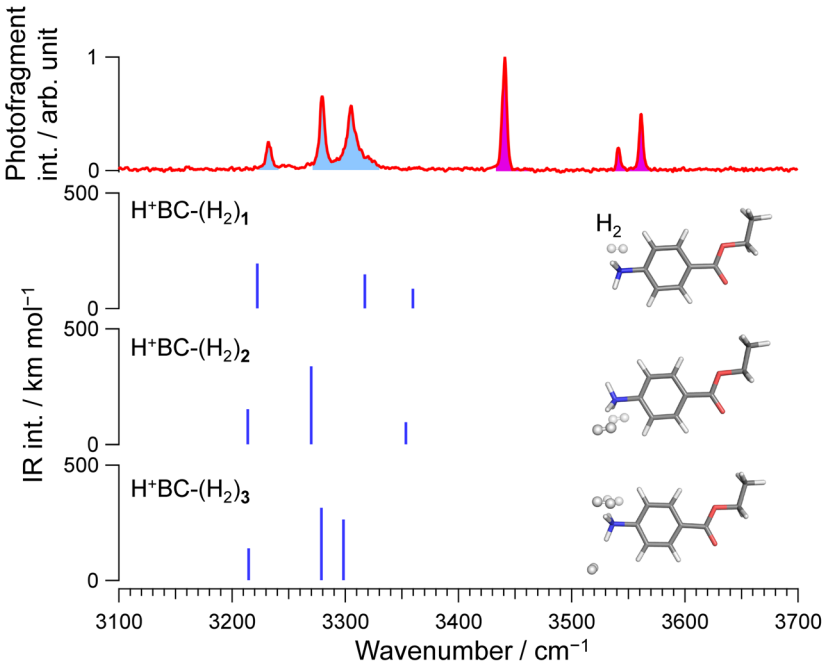

Figure S11. Calculated IR spectra of the H_2-tagged N-protomer at the ωB97X-D/6-311++G(d,p) level compared with the CAS-IRPD spectrum of $H^+BC(H_2O)_3$.

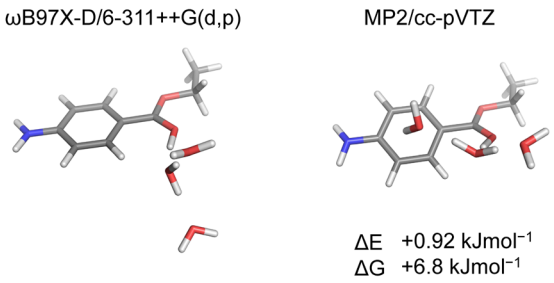

Figure S12. Optimized structure of the O-protomer of $H^+BC(H_2O)_3$ at the MP2/cc-pVTZ level compared to the structure obtained at the ωB97X-D/6-311++G(d,p) level. The obtained MP2 structure is different from the one obtained for ωB97X-D. Although the electronic energy (ΔE) of the structure is close to the N-protomer, the structure is less stable in ΔG due to entropy. The structural optimization was programmed to minimize the electronic energy and thus conformational search on a free energy surface is needed. This is highly challenging for floppy system such as hydrated clusters.

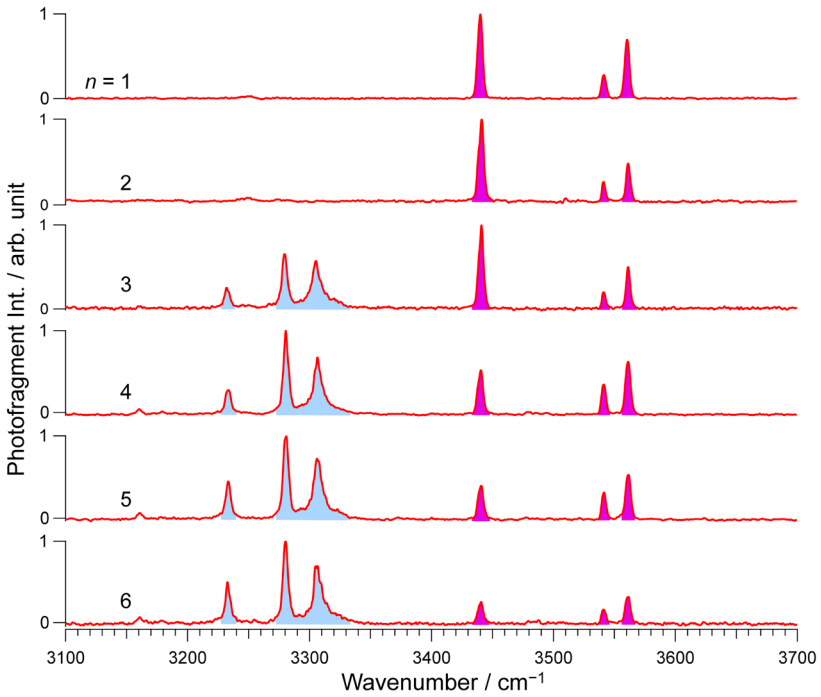

Figure S13. CAS-IRPD spectra of $H^+BC(H_2O)_n$ (n=1-6). The difference in relative photofragment intensities for the O-protomer bands (3441 and 3561 cm^{-1}) may arise from the saturation of photoabsorption in the n = 4-6 spectra.

Table S1. Experimentally obtained relative population of the N-protomer in $H^+BC(H_2O)_n$ compared to theoretical values using different functionals (ωB97X-D, B3LYP-D3, M06-2X) with the same basis set (6-311++G(d,p)) and *ab initio* MP2 calculations.

n	Exp. (%)	Calc. (%)			
		ωB97X-D	B3LYP-D3	M06-2X	MP2
1	0	0	0	0	—
2	0	0	0	0	—
3	63(11)	13	0	0	99

References

(1) Ishiuchi, S.; Wako, H.; Kato, D.; Fujii, M. High-cooling-efficiency cryogenic quadrupole ion trap and UV-UV hole burning spectroscopy of protonated tyrosine. *J. Mol. Spectrosc.* **2017**, *332*, 45-51.

(2) Suzuki, Y.; Hirata, K.; Lisy, J. M.; Ishiuchi, S.; Fujii, M. Double Ion Trap Laser Spectroscopy of Alkali Metal Ion Complexes with a Partial Peptide of the Selectivity Filter in K^+ Channels─Temperature Effect and Barrier for Conformational Conversions. *J. Phys. Chem. A* **2021**, *125*, 9609-9618.

(3) Marsh, B. M.; Voss, J. M.; Garand, E. A dual cryogenic ion trap spectrometer for the formation and characterization of solvated ionic clusters. *J. Chem. Phys.* **2015**, *143*, 204201.

(4) Frisch, M. J.; Trucks, G. W.; Schlegel, H. B.; Scuseria, G. E.; Robb, M. A.; Cheeseman, J. R.; Scalmani, G.; Barone, V.; Petersson, G. A.; Nakatsuji, H., et al., Gaussian 16 Revision B.01 J. Gaussian, Inc., Wallingford CT, 2016.

(5) Chang, T. M.; Prell, J. S.; Warrick, E. R.; Williams, E. R. Where's the charge? Protonation sites in gaseous ions change with hydration. *J. Am. Chem. Soc.* **2012**, *134*, 15805-15813.

(6) Voss, J. M.; Marsh, B. M.; Zhou, J.; Garand, E. Interaction between ionic liquid cation and water: infrared predissociation study of $[bmim]^+\cdot(H_2O)_n$ clusters. *Phys. Chem. Chem. Phys.* **2016**, *18*, 18905-18913.